SINTERING OF ALUMINA—MOLYBDENUM COMPOSITES CONTAINING CALCIUM—ALUMINOSILICATE GLASS

by

PRASANTA PANIGRAHI

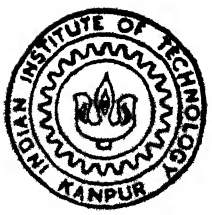

MATERIALS SCIENCE PROGRAMME

INDIAN INSTITUTE OF TECHNOLOGY KANPUR

August, 1992

SINTERING OF ALUMINA—MOLYBDENUM COMPOSITES CONTAINING CALCIUM—ALUMINOSILICATE GLASS

A Thesis Submitted
in Partial Fulfilment of the Requirements
for the Degree of

MASTER OF TECHNOLOGY

by

PRASANTA PANIGRAHI

to the

MATERIALS SCIENCE PROGRAMME

INDIAN INSTITUTE OF TECHNOLOGY KANPUR

August, 1992

10.8.92

CERTIFICATE

This is to certify that the thesis entitled 'SINTERING OF ALUMINA-MOLYBDENUM COMPOSITES CONTAINING CALCIUM-ALUMINOSILICATE GLASS' submitted by Mr. Prasanta Panigrahi has been carried out under my supervision and has not been submitted elsewhere for a degree.

8/8/92
August, 1992

G.S. UPADHYAYA
Professor
Department of Metallurgical Engineeri
Indian Institute of Technology
Kanpur 208016

MSP-1992-M-PAN-SIN

ACKNOWLEDGEMENTS

I wish to express my profound sense of gratitude to Prof. G.S. Upadhyaya for his excellent guidence and inspiration in every step of this work.

I also thank all my lab mates i.e. Mr. S.K. Bhowmik, Mr. H.N. Azari, Mr. N. Kapuri and Mr. Govind for their cooperation and encouragement.

The help rendered by Mr. Santanu Bhattacharya, Mr. S. B. Majumdar, Mr. A. Saha, Mr. B. Saha and Mr. B. Ghosh will be remembered for ever.

Special thanks to all staffs of ACMS and MSP for their help and cooperation.

Finally I thank Mr. S.K. Srivastava for his neat typing.

(Prasanta Panigrahi)

CONTENTS

LIST OF FIGURES

ABSTRACT

The present investigation deals with solid and liquid phase sinterings of alumina-molybdenum composites. For liquid phase sintering a calcium-aluminosilicate glass was prepared by melting an eutectic mixture of the respective powders. Three batches of powder mixtures containing alumina-0, 5 and 10 mass % glass were prepared and to each batch, 0-16 mass % molybdenum was added. All the specimens were processed using the powder metallurgy technique. The green pellets were sintered at 1400^{o}C for 30 minutes in hydrogen atmosphere. The straight alumina-molybdenum composites were again sintered at 1650^{o}C for one hour in air.

The liquid phase sintered composites were found to have increasing density with addition of molybdenum and/or glass. The molybdenum addition decreases the grain growth of alumina matrix. These features were correlated with the mechanical properties of the composites.

In case of solid state sintering, at 1650^{o}C, molybdenum addition enhances sintered density and mechanical properties. Considerable grain growth was also observed in the solid state sintered alumina-molybdenum composites. A maximum sintered density (89% theoretical) were obtained for Al_2O_3-8 % Mo composition.

CHAPTER - I

LITERATURE REVIEW

I.1. INTRODUCTION:

Alumina is the most extensively studied ceramic material due to its excellent properties such as high compressive and tensile strength, high hardness, high rigidity, high thermal shock resistance, low thermal expansion coefficient etc. The use of α-alumina as an advanced structural ceramic material has imparted tremendous success due to its added beneficial properties such as chemical inertness, corrosion resistance, low friction coefficient, phase stability upto high temperature and above all its retention of mechanical properties at high temperature [1].

Despite all these, the property most disadvantageous for its use as a structural material is its brittleness. Much research has been carried out since last few decades to overcome this hinderance by studying the fracture behaviour of polycrystalline alumina ceramics. For brittle polycrystalline ceramics (e.g. Alumina), it is well understood that the fracture strength is limited to flaws and internal stresses as suggested by Griffith [2]. It is also seen by Petch [3] that the fracture strength decreases with increasing grain size of the ceramics. To decrease the brittleness i.e. to increase the toughness of the polycrystalline ceramics much effort has been made using several methods such as particle toughening, transformation toughening, compressive surface stress,

microcracking etc. [4]. The present work deals with the first method i.e. particle toughening of alumina by incorporating molybdenum metal particles.

Similar to metals, attempts has been made to increase the strength of ceramics by the incorporation of second phase particles. Both ceramic and metal phases have been used for this purpose. The basic mechanism of particle toughening is to impede the crack front by pinning it at the inclusions. As suggested by Lange [5] and Evans [6], the increase in fracture toughness or fracture energy depends upon the size, shape and concentration of the second phase. The strengthening effect is due to the bowing of crack line between two pinning obstacles. Since the crack front can be treated as having a line energy per unit length, crack front bowing means consumption of additional energy, which must be supplied by the elastic stress field ahead of the crack front, thereby leading to an increasedvalue of fracture energy at the moment of breakaway. The dispersion of metallic phase in the ceramic matrix (i.e. Alumina) imparts an added advantage as more energy of the crack front is consumed by the plastic deformation of the metallic phase.

I.2. MATERIAL SELECTION:

The nature of both the ceramic and metallic phase and their mutual interaction is the most important factor affecting the fabrication and properties of ceramic-metal composite [7]. The bonding between the two phases depends upon the reaction involving the time, thermal expansion coefficients,

surface and interface energy etc. A decrease in interfacial energy or mutual solubility between the two phases results strong bonding between the two.

The first report of alumina-molybdenum cermet preparation came from McHugh et al. [8], where the incorporation of molybdenum particles enhanced the strength of the composite due to strong bonding between the two. The coefficients of linear thermal expansion of alumina and molybdenum match well even at high temperature (Figure I.1). The experiments done so far on this system, which will be reviewed subsequently, show that the sintering temperature required for the preparation of alumina-molybdenum cermet is quite high (1650°C approximately). As there is no such literature available on the liquid phase sintering of this system, liquid phase sintering of pure alumina will be reviewed subsequently.

I.3. POWDER PREPARATION AND CHARACTERISATION:

As described earlier, the size and shape of the dispersed particle effect the properties of the composite. Also, fine powder of the ceramic phase is advantageous as it lowers the sintering temperature and yields a fine grain size structure improving the mechanical properties.

For the preparation of Al_2O_3-Mo cermet, usually, the powder metallurgy route is employed where alumina and molybdenum powders are directly used. McHugh et al. [8] prepared the batch of powder mixture from alumina and molybdenum powders directly. Another method employed by them was to reduce the powder mixture of alumina and MoO_3 above 800°C in dry hydrogen

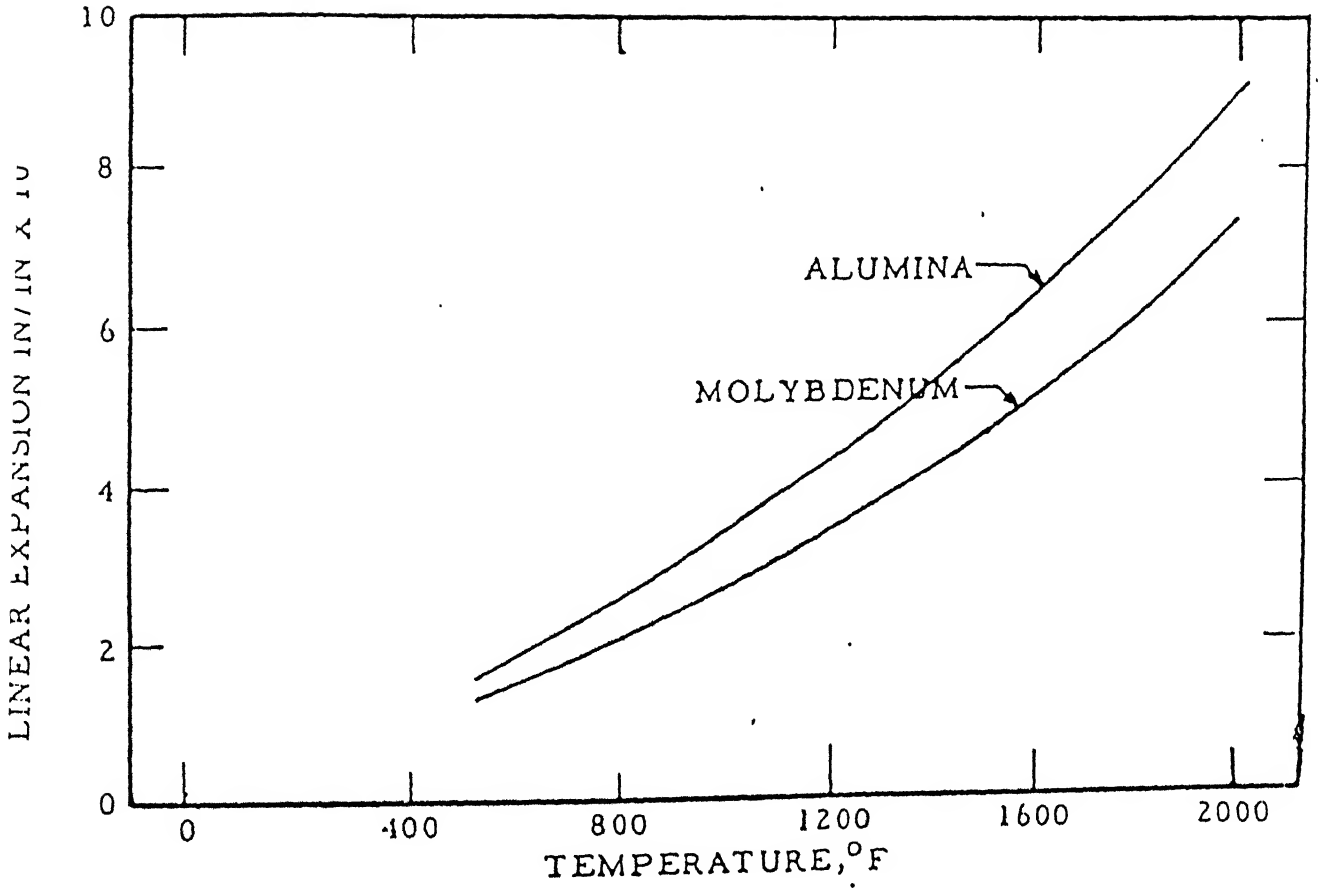

Fig. I.1 Variation of linear thermal expansion of alumina and molybenum with temperature.

atmosphere. Most of the researchers followed the first method for the batch preparation for fabrication of alumina-molybdenum cermet [9-13]. Raman [14] prepared the powder mixture through sol-gel technique, by mixing individual sol of aluminium and molybdenum producing Al-Mo hydroxide gel, which was subsequently dried and used for compaction.

I.4. DENSIFICATION BEHAVIOUR:

I.4.1. Pure Alumina Densification:

In conventional powder metallurgy route, densification involves two steps of processing i.e. green compaction and sintering. Green compaction involves applying pressure on the alumina powder kept inside a die (usually made of steel) so as to give the green body a shape and strength for subsequent handling. The most important phenomenon in this step is the formation of bridge between the particles by increasing the contact surface. An increase in contact area between the particles helps better diffusion which increases its sinterability. Hence an increase in green density increases the sintered density.

Sintering is the most important step of processing for the fabrication of ceramic body, which determines its final properties. Densification, grain growth and recrystallisation occur in the same temperature range of alumina sintering. The density increases with time and grain size increases with one-third power of time [15].

Increase in ball milling time of alumina powder or sintering temperature improves the densification kinetics but

for higher ball milling time, increase in sintering temperature does not improve the sintered density [16]. Johnson and Cutler [17] found that plot of logarithm shrinkage Vs. logarithm time appeared to become straight after an initial curvature. A further study on sintering kinetics of alumina by Kuczynski et al. [18] revealed that the process of sintering was one of the volume diffusion regardless the kind of sintering atmosphere. It was also established that sintering in dry hydrogen atmosphere was much faster than that in any other atmosphere due to the creation of oxygen vacancy or interstitial aluminium atom.

Yeh and Sung [19]; Xue and Chen [20] sintered slip cast cakes containing submicron size alumina powder at temperature as low as 1250^{o}C to achieve more than 98% theoretical density.

I.4.2. Alumina-Glass Densification:

The densification behaviour of alumina-glass system depends upon the nature and amount of the glass melt present during sintering. According to the nature of driving force acting during sintering Kingery [21] has classified the process into three stages i.e. (1) Particle rearrangement, (2) Solution reprecipitation and (3) Particle coarsening. He has also proposed that solution precipitation does not lead to 'centre to centre' approach, a necessary condition for shrinkage. Experimental evidence showed that sintering did not occur in discrete stages but several processes were present throughout the entire sintering process. Singh [22] and

Kingery [23] examined the liquid phase sintering of alumina and concluded that their results were not consistent with Kingery's original model. Agrawal and Narasimhan [24] found that there was an optimum liquid phase content for producing maximum densification of alumina. They also observed that increase in liquid phase content increased the grain growth rate. The densification rate increased with increasing liquid phase content, as observed by Kwon and Messing [25]. The effect of particle size of alumina on the sintering rate was studied by Flaitz [26], Hodge [27] and Kwon and Messing [25] who found the rate of sintering increased with decreasing particle size of alumina powder. Kostic and Boskovic [28] found that the influence of various dopents on densification depended upon the types of reaction product formed during the formation of liquid phase. They also concluded that addition of a liquid phase in equilibrium with alumina at sintering temperature favourably effected the sintering process.

I.4.3. Al_2O_3- Mo Densification:

The densification behaviour of alumina-molybdenum depends mostly upon the initial powder characteristics, amount and distribution of the metallic phase. The solid state sintering of such systems is carried out either in hydrogen atmosphere or in vacuum. The effect of sintering atmosphere is also significant along with the processing parameters towards achieving a dense sintered alumina-molybdenum cermet.

Mc Hugh et.al. [8] found that Al_2O_3-Mo alloy densified more slowly than pure alumina during the initial period of

sintering, which at the end of 60 minutes attained the relative density same as that of pure alumina. Alumina-molybdenum composites containing MgO as a grain growth inhibitor were hot pressed to near theoretical density by Rankin et al. [9]. All the samples containing upto 5 vol % Mo were found having not much difference in sintered density due to MgO addition. Fidotov [13] found that the relative sintered density of alumina-molybdenum cermet increased with molybdenum content, upto 10 vol %. He also observed that a slight decrease in the degree of dispersion of molybdenum adversely affected the densification. Fidotov and Lutskaya [12] found that above 20 wt % molybdenum content in the cermet increased the porosity i.e. decreased the sintered density. Also the sintering in moist hydrogen atmosphere was found to be more active with respect to that in the dry hydrogen atmosphere.

I.5. MICROSTRUCTURAL CHARACTERISTICS:

Mc Hugh et.al. [8] found that with increasing amount of molybdenum content in the Al_2O_3-Mo cermet the grain size of Al_2O_3 decreases. The grain size is not affected with the increase in molybdenum content above 5 vol %. No agglomeration was seen upto 5 vol % molybdenum. Microstructures, of the cermets prepared from powder obtained by different methods, were almost same.

In a sample containing Al_2O_3-3 vol % Mo, Rankin et al. [9] showed that the metal phase was distributed evenly. But they found that molybdenum addition to Al_2O_3 did not help grain refinement. MgO inhibited grain growth of Al_2O_3 with

or without the presence of molybdenum phase. This disagrees with the work of Mc Hugh et al. [8]. Most of the molybdenum particles were seen at the Al_2O_3 grain boundary, though some amount had been seen within the large Al_2O_3 grains.

Al_2O_3-Mo cermet developed by Raman [14] appeared to decorate the grains and grain boundary. Besides being randomly scattered they were linearly arranged. Molybdenum particles were also seen in the core of triangular pits which were seen both in free and fracture grain surfaces. Some of the molybdenum particles were found to be overgrown.

Molybdenum particles inhibited grain growth as established by Fedotov [13]. Alumina particles grew in the region mainly devoid of molybdenum phase. The molybdenum particles had an elongated sinous shape.

The microstructure of liquid phase sintered alumina depends upon the nature of liquid phase present during sintering. Agrawal and Narasimhan [24] observed considerable grain growth of alumina as the amount of liquid phase was increased. They found the grains of alumina in prismatic shape. Kaysser et al. [29] found that the addition of anorthite and MgO decreased growth rate of alumina matrix with comparison to undoped alumina. It was also observed that the addition of anorthite with or without MgO single crystal seeds exhibited basal facets. Kwon and Messing [25] examined the microstructural changes occurring during solution-reprecipitation stage which revealed that during initial period the particle contacts were relatively narrow which subsequently became flattened indicating the process of extensive solution reprecipitation.

The individual particle shapes remained prismatic. Hodge [27] carried out the experiment with both wide and narrow range particle size distributed alumina powder. The powder with wide particle size distribution revealed equiaxed grains when sintered at 1475°C and flat sided platelike grains with faceting behaviour when sintered at 1625°C. Similar trend was also observed in the narrow particle size distributed powder. Song and Coble [30] observed platelike grain structure in the liquid phase sintered samples which was dependent upon the dopant cation ion size and valency.

I.6. MECHANICAL BEHAVIOUR:

I.6.1. Hardness:

Microhardness measured by Rankin [2] was about 2215 Kg/mm^2 to 1910 Kg/mm^2 for alumina compacts containing 1 vol % molybdenum to 5 vol % Mo. With MgO addition in each composition the microhardness increased by an amount of 40 to 50 Kg/mm^2.

The Vickers hardness of sintered alumina as determined by Brokhin et.al. [4], increased with decreasing amount of molybdenum. They found that the hardness varied linearly with molybdenum content from 180 HV for pure molybdenum to 1800 HV for pure alumina.

I.6.2. Transverse Rupture Strength (TRS):

The transverse rupture strength with respect to the molybdenum content in the alumina-molybdenum cermet showed that a progressive increase in strength occurred with increase in

molybdenum content upto 5 vol % . McHugh et al. [8] showed that a progressive increase in TRS occurred with increase in molybdenum content upto 5 vol %. They supported the result with the fact that the grain size decreased as the molybdenum content increased. They found TRS for pure alumina and alumina with 5 vol % molybdenum as 361.7 MPa and 800 MPa respectively.

Skidan et.al. [10] found the TRS values of 10 wt % Mo and 30 wt % Mo to be 243 MPa and 203.3 MPa respectively. Also at 1000^{o}C the TRS values for the above two compositions were 142 MPa and 159 MPa respectively.

I.6.3. Fracture Behaviour:

Fracture in alumina-molybdenum cermet is intergranular in nature. The fracture strength depends upon the bonding between the two phases as well as the microstructure of the composite. The distribution of metallic phase in the matrix is also vital for determining the fracture strength or toughness. Raman [14] found the fracture energy and fracture toughness value of the Al_2O_3-5 vol % Mo composite to be 58.5 joul/m^2 and 6.73 MPa $\sqrt{m}$ respectively. The fracture energy and fracture toughness values were almost 50% higher than those of pure alumina.

I.7. SCOPE OF THE PRESENT INVESTIGATION:

To enhance the sinterability and mechanical properties of polycrystalline alumina ceramics, incorporation of various second phases were investigated by various authors. As

described earlier, molybdenum addition has been successful in enhancing the densification as well as the mechanical properties of alumina. Its influence on the microstructure is most significant which inhibits the grain growth of the matrix. In the present investigation alumina-molybdenum cermet preparation has been carried out through powder metallurgy route. The aim of the experiment is to study the sintering behaviour of the composite.

As reviewed earlier, the alumina-molybdenum cermet sintering is purely solid state in nature and the interaction between the two involves no chemical reaction and therefore the sintering temperature required is quite high. To decrease the sintering temperature, a glassy phase has been added to the system for liquid phase sintering.

CHAPTER - II

EXPERIMENTAL PROCEDURES

II.1. POWDER CHARACTERIZATION:

For the preparation of alumina-molybdenum cermet, conventional powder metallurgy route viz. milling, compaction and sintering was followed. The alumina powder used was obtained from M/s Indian Aluminium Company, Belgaum, India (HMT 30 Grade). The molybdenum powder was supplied by Metallwerk, Plansee, Austria. The specific gravities of the alumina and molybdenum powders were found to be 3.95 gm/cc and 10.22 gm/cc respectively.

The particle size analysis of alumina and molybdenum powder was carried out using Coulter Counter model Z_B and B (Coulter Electronics Ltd., England). The experimental parameters for these measurements are given below:

Experimental Parameters Used in Particle Size Analysis

	For Aluminium	For Molybdenum
Electrolyte	NaCl	NaCl
Aperture diameter	50 μm	140 μm
Manometer volume	0.05 μl	0.5 μl
Calibration factor	1.51	3.18
Dispersent	Coulter	Coulter
Grain control	5	5
Matching switch	10	10

II.2. GLASS POWDER PREPARATION:

An eutectic composition of $CaO-Al_2O_3-SiO_2$ system was selected for the glassy phase preparation. CaO was obtained by calcining $CaCO_3$ powder. Al_2O_3 and SiO_2 powders were taken in pure form. The composition selected was as follows:

Al_2O_3 - 14.7 wt %

CaO - 23.3 wt %

SiO_2 - 62%

The eutectic composition is shown in the ternary phase diagram of Figure II.1. The eutectic melting temperature of the above composition is 1170°C [31]. The constituent powders (viz. Al_2O, SiO_2 and CaO) were mixed manually in morter pastle, according to their weight percentage, thoroughly Then the powder mixture was melted at 1400°C in an alumina crucible for 2 hours, so that the glass melt gets homogenised and free from gaseous inclusions.

The furnace used for melting was a resistance heated SiC pit furnace. The glass melt was furnace cooled to room temperature. The glass lump thus obtained was extracted mechanically from the crucible and crushed into a coarse powder form. This powder was ball milled for 24 hours in porcelain jar in water medium using alumina balls of approximately 2 cm diameter. The fine powder thus obtained was dried and sieved through 325 mesh size to obtain -44 μm particle size powder.

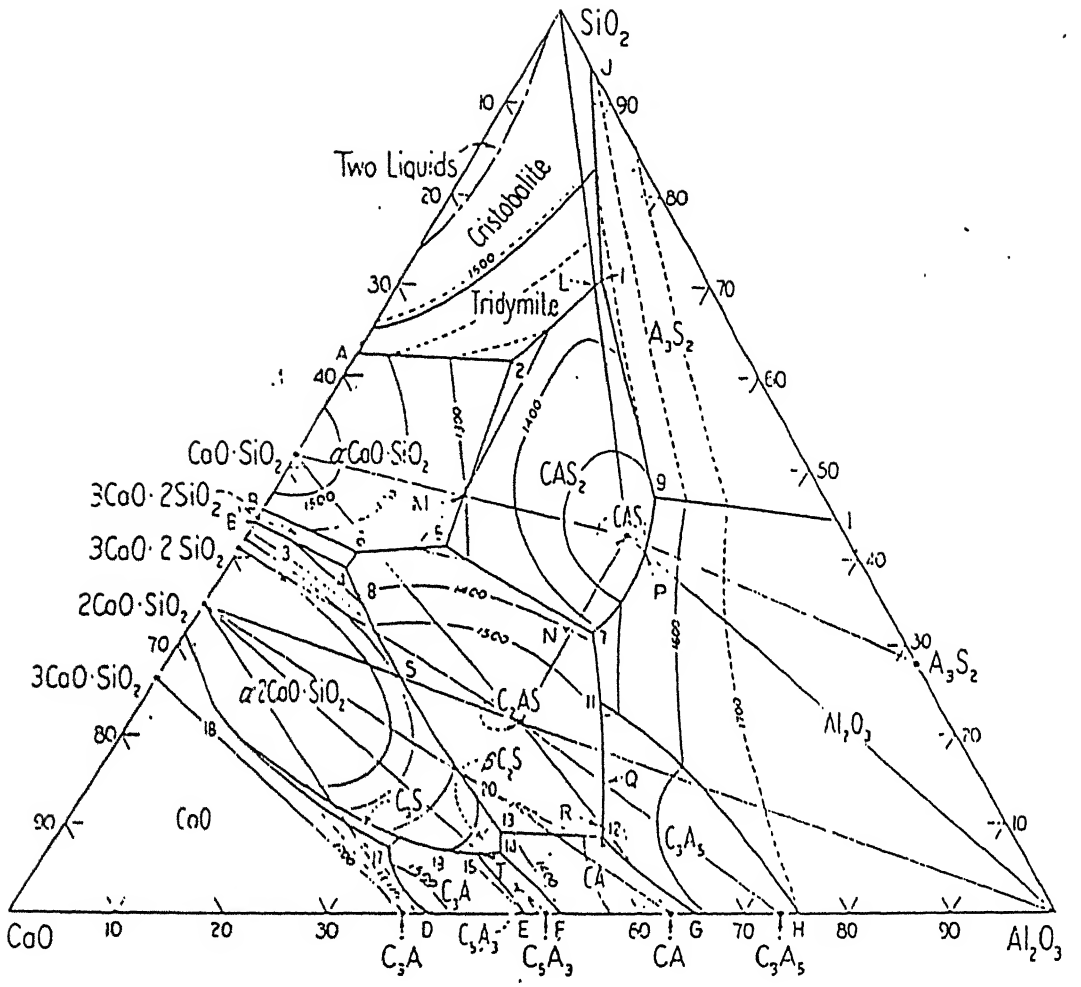

Fig. II.1 Equillibrium phase diagram of CaO-Al_2O_3-SiO_2 ternary system [31].

II.3. BATCH PREPARATION:

To prepare alumina-glass samples, 0-20 wt % glass powder was added to alumina powder at a regular interval of 5 wt %. The dry mixing was done in a laboratory double cone blender for one hour.

Molybdenum powder was added to the alumina-glass powder mixture obtained as above, and its content was varied from 0-16 wt % at an interval of 4 wt %. The mixing was carried out manually in an agate morter for 2 hours in acetone medium. The powder mixtures were thus dried on an electrically heated oven at 80°C.

II.4. GREEN COMPACTION:

The powder mixtures were compacted in a high carbon high chromium steel die of rectangular shape. The approximate green dimension of the pellets was about 4.5 cm X 1.5 cm X 0.4 cm. Prior to each filling of powder the die and punches were cleaned by acetone. A pressure of 175 MPa was applied by using a manually operated single acting hydraulic press.

Polyvinyl alcohol solution (PVA) of 1% concentration was used as binder to give enough strength to the green pellets for subsequent handling. The pellets thus obtained were dried at 105 $\pm$ 5°C.

II.5. SINTERING:

The green pellets were sintered in a SiC resistance heated tubular furnace at 1400°C $\pm$ 5°C for 30 minutes under a dry hydrogen atmosphere. The dew point of the hydrogen gas

was measured using a Shaw moisten meter (U.K. made) and was found to be around -35°C. The heating rate was around 8°C/min. The hydrogen used as atmosphere was dried and cleaned by passing through a purification train before introducing it into the furnace. The hydrogen purification train consisted of a hydrogen purifier (DEOXO, Model 0.15/3.5 of Glouc ster-shire, U.K.) tubes containing calcium chloride for drying and glass wool/cotton for removing any suspended particles.

The sintered Al_2O_3-Mo samples without any glass content were resintered in air at still higher temperature of 1650°C ± 5°C for one hour. The furnace used was muffle type and the heating rate were kept about 3°C/min.

II.6. CHARACTERIZATION:

II.6.1. Density Measurements:

All the dried samples prior to sintering were weighed and their dimensions were measured for the evaluation of green density.

Sintered density of all the samples was determined by Archemedis principle [32]. At first the sintered pellet was weighed in air (W_1). Then the sample was suspended in water under vacuum for half an hour so that water get impregnated inside the open pores of the sample. The water impregnated samples surface was cleaned and weighed again in air (W_2). Finally, the sample's weight was taken while in suspension in water (W_3). For the density calculation, the following formula was used:

$$\text{Sintered density, } D = \frac{W_1}{W_2 - W_3} \qquad (2.1)$$

where D is expressed in gm/cc and W_1, W_2 and W_3 in grams.

Theoretical density of all the compositions were calculated by using the rule of mixture. Sintered density of all samples were expressed in terms of relative density (% theoretical) by dividing the sintered density by theoretical density.

II.6.2. Transverse Rupture Strength (TRS):

The transverse rupture strength of the samples was determined by three point bending test as per ASTM specification (B406-76). The sample size was 4.40 cm X 1.40 cm X 0.3 cm approximately. The load at rupture was determined by using a 100 KN Instron 1195 system testing machine. A 1000 Kg load cell was used with a crosshead speed of 0.05 mm/min. The span length of the TRS fixture was 3 cm. The full scale load and chart speed were 20 Kg and 100 mm/min respectively. The TRS valuesof the samples were calculated using the following formula:

$$TRS = \frac{3PL}{2WD^2} \qquad (2.2)$$

where TRS = Strength, MPa

P = Rupture load, MN

L = Span length, m

W = Width of the specimen, m

D = Depth of the specimen, m.

II.6.3. Vickers Hardness:

For the measurement of Vickers hardness, all samples were polished using 1 μm size diamond paste. The indentation was done at a load of 10 Kg, randomly. The indentation diagonals were measured by the help of a travelling microscope and the average length was calculated. The Vickers hardness value was found out from the hardness table at 10 Kg load.

II.6.4. Fracture Toughness (K_{IC}):

Plain strain fracture toughness (K_{IC}) was determined by using the 'Single Edge Notch Beam' (SENB) method [33]. The sintered samples were cut to a size of 1.5 cm X 0.7 cm X 0.2 cm with the help of diamond saw. The samples were notched with the help of a sharp diamond blade of 0.3 mm thickness. The notch length was made in the range of 0.35 to 0.55 of the sample depth. Three point bending test was followed to determine the fracture toughness (K_{IC}). A 100 KN capacity Instron machine was used to evaluate the load at fracture. The span length was kept at 1.5 cm. A 1000 Kg load cell was used with a crosshead speed of 0.05 mm/min. The fracture toughness was calculated using the following formula [33]:

$$K_{IC} = \frac{3PLC^{1/2}}{2WD^2}\left[A_0 + A_1\left(\frac{C}{D}\right) + A_2\left(\frac{C}{D}\right)^2 + A_3\left(\frac{C}{D}\right)^3 + A_4\left(\frac{C}{D}\right)^4\right] \quad (2.3)$$

where K_{IC} = Fracture toughness, MPa $\sqrt{m}$

P = Fracture load, MN

L = Span length, m

C = Notch length, m

W = Width of the sample, m

D = Depth of the sample, m.

When $C \simeq \frac{D}{2}$

$$A_0 = 1.90 + 0.0075 \left(\frac{L}{D}\right)$$

$$A_1 = -3.39 + 0.08 \left(\frac{L}{D}\right)$$

$$A_2 = 15.4 - 0.2175 \left(\frac{L}{D}\right)$$

$$A_3 = -26.24 + 0.2815 \left(\frac{L}{D}\right)$$

$$A_4 = 26.38 - 0.145 \left(\frac{L}{D}\right)$$

II.7. X-RAY DIFFRACTION ANALYSIS:

X-ray diffraction patterns of all the sintered samples were taken with REICH-SEIFERT ISO-DEBYFLEY 2002 diffractometer. The study was also carried out with alumina, molybdenum and glass powder. The X-ray used was CuK_α radiation. The scanning speed and counts per minute were 3^o/min and 10 K respectively.

II.8. SEM FRACTOGRAPHY:

The fractured surface of the sintered samples were observed with the help of scanning electron microscope (JEOL, JSM 840A, Japan). The fractured surface, after washing in acetone, was silver coated in a coating unit at a vacuum of 0.1 torr to ensure conductivity. Secondary electron images of the surface were photographed to observe the grain size, distribution of molybdenum in the alumina matrix and the fracture characteristics.

CHAPTER - III

RESULTS

PART-A: Liquid Phase Sintered Composites

III.1. POWDER CHARACTERISTICS:

The particle size distributions of alumina and molybdenum powders, used for the composites preparation, are shown in Fig. III.1, which revealed that the alumina powder was much finer than molybdenum powder. The mean particle sizes of the two powders were determined to be 2 μm and 10 μm for alumina and molybdenum powders respectively.

III.2. DENSITY:

The green density of the pellets of all samples were found to be nearly same having a magnitude of 54% theoretical. Fig. III.2 shows the variation of sintered density with glass content in the alumina-glass composites. It shows that addition of glass to alumina does densify the liquid phase sintered composites and upto 10 wt % glass, increase in glass content increases the sintered density. At 10 wt % of glass the sintered density reaches its optimum value of 70% theoretical and as the glass content increases the sintered density decreases gradually.

The addition of molybdenum to alumina improves densification as shown in Fig. III.3. The addition of 5 and 10 mass % glass in Al_2O_3-Mo composites further improves the

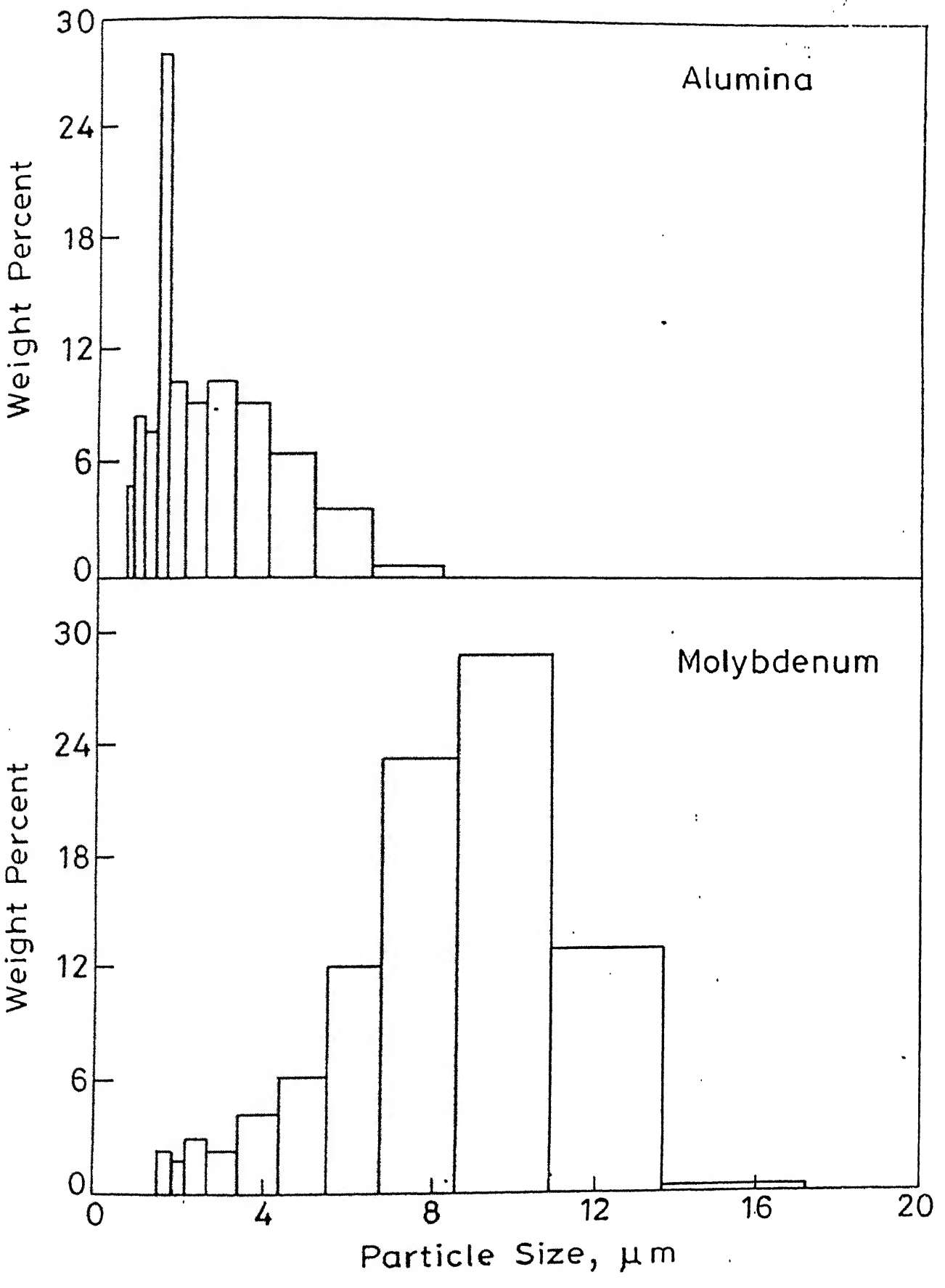

Fig. III.1 Partical size distributions of alumina and molybdenum powders.

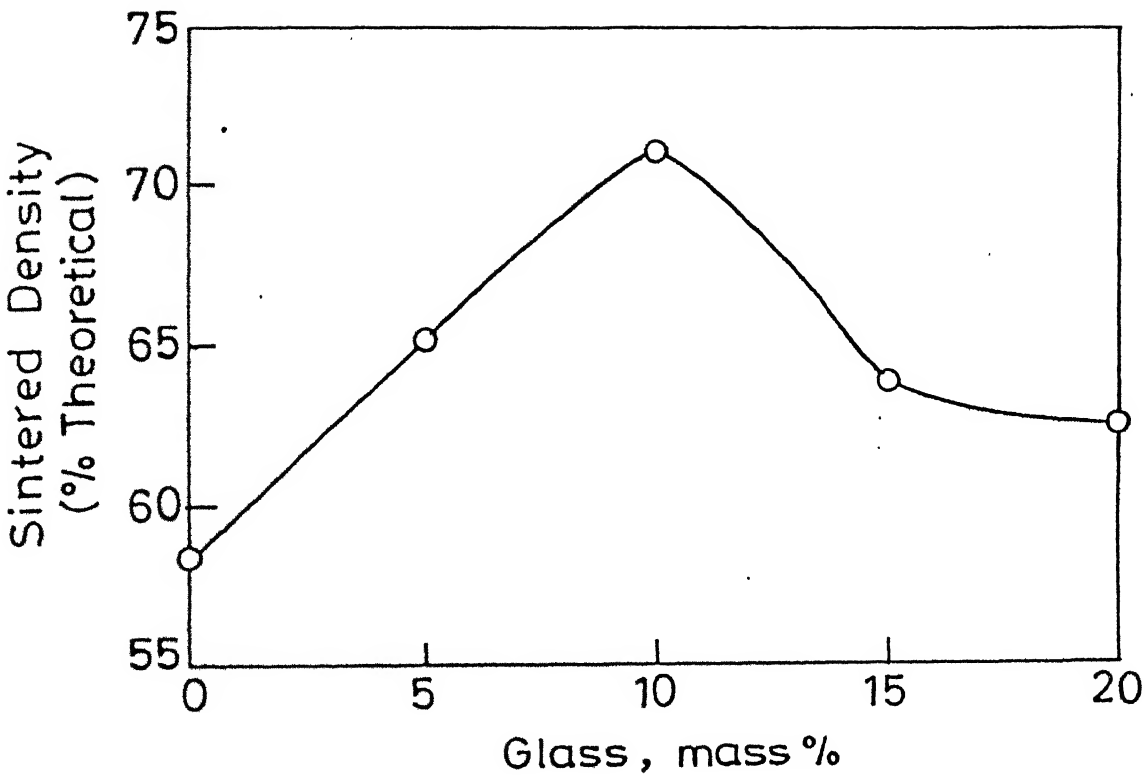

Fig. III.2 Variation of sintered density (% theoretical) with glass content of alumina-glass composites.

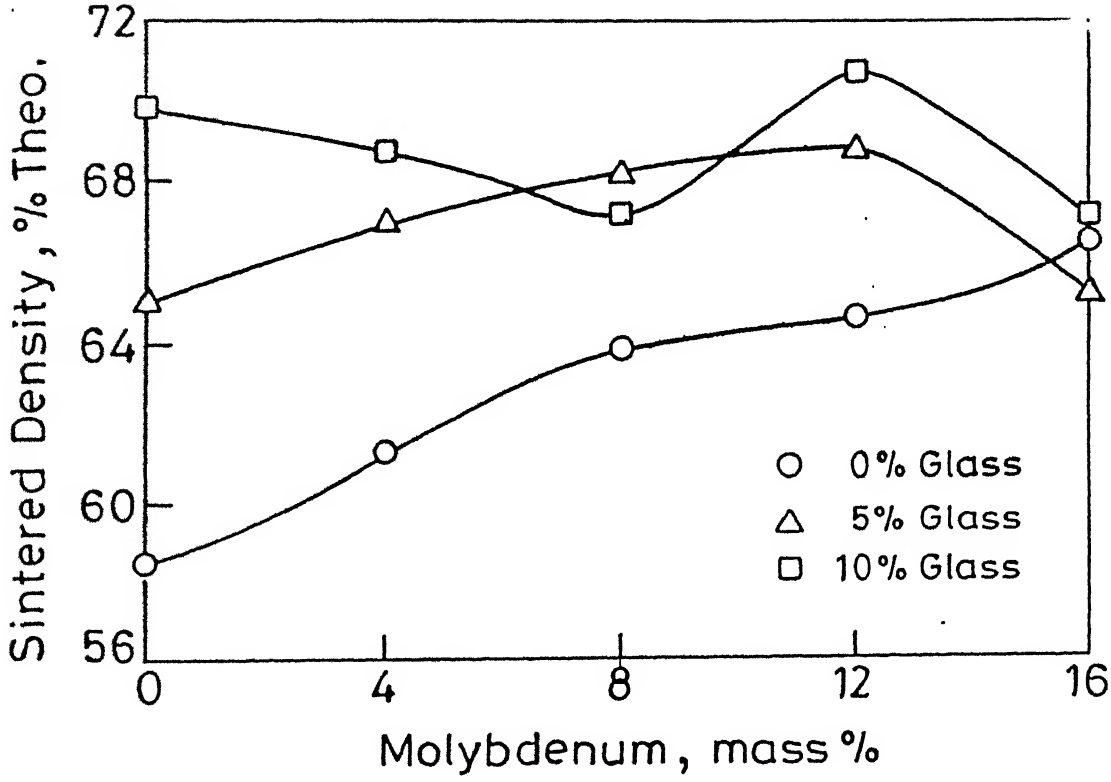

Fig. III.3 Variation of sintered density (% theoretical) with molybdenum content of alumina molybdenum-glass composites.

sintered density. In 5 and 10 mass % glass containing composites, the sintered density of 16% molybdenum containing composition got decreased, so as to attain the values of 0% glass composition. The enhancement of sintered density for 10 mass % glass containing composites was less significant with respect to that for 0 and 5 mass % glass containing composites

III.3. MECHANICAL PROPERTIES:

III.3.1. Transverse Rupture Strength (TRS):

Fig. III.4 shows that the addition of molybdenum to all the glass containing composites improves TRS also. The variation of TRS with molybdenum content in the composites has the same trend as that of density. The enhancement of strength with glass addition to the Al_2O_3-Mo composites was found more significant for lower molybdenum content than that for higher molybdenum content. Among various molybdenum containing composites, alumina 5 mass % glass composition gave rise to a higher strength than any other compositions.

III.3.2. Vickers Hardness:

Vickers hardness variation of the sintered samples tend to follow the same trend as that of TRS (Fig. III.5). The hardness of 0 and 5 mass % glass containing composites were found increasing with molybdenum addition unlike that of 10 mass % glass containing composites.

III.3.3. Fracture Toughness (K_{IC}):

Fracture toughness variation with molybdenum content

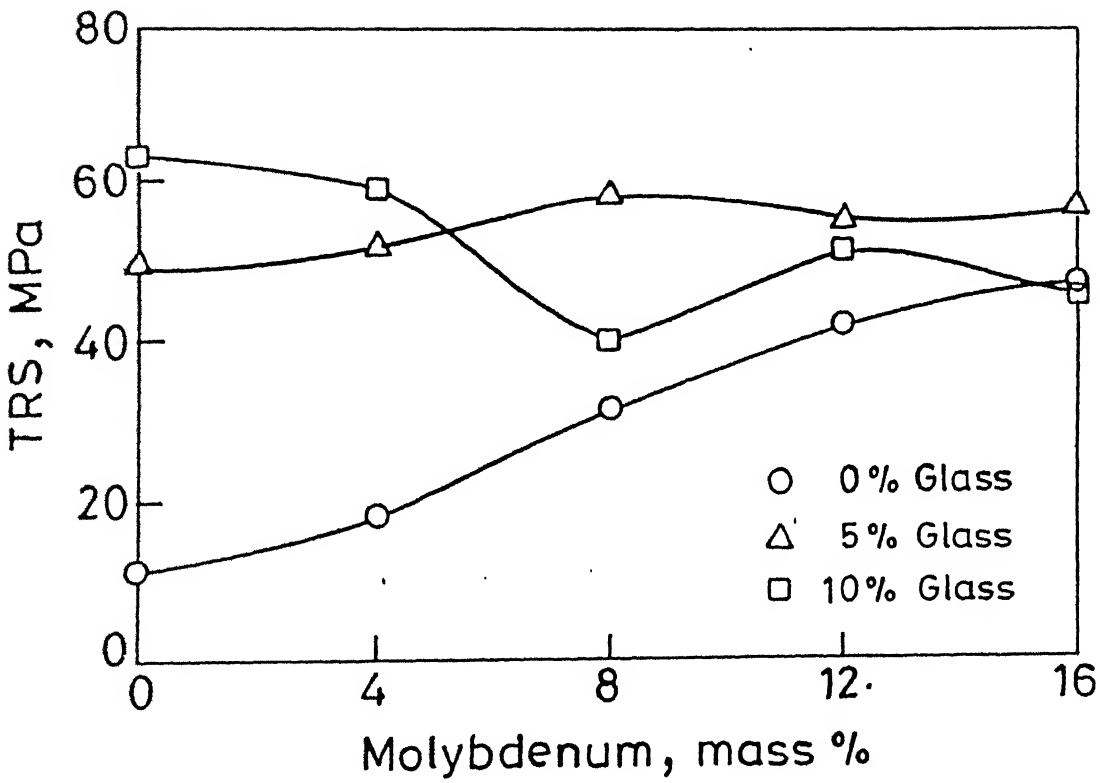

Fig. III.4 Variation of TRS with molybdenum cont
of alumina molybdenum-glass composit

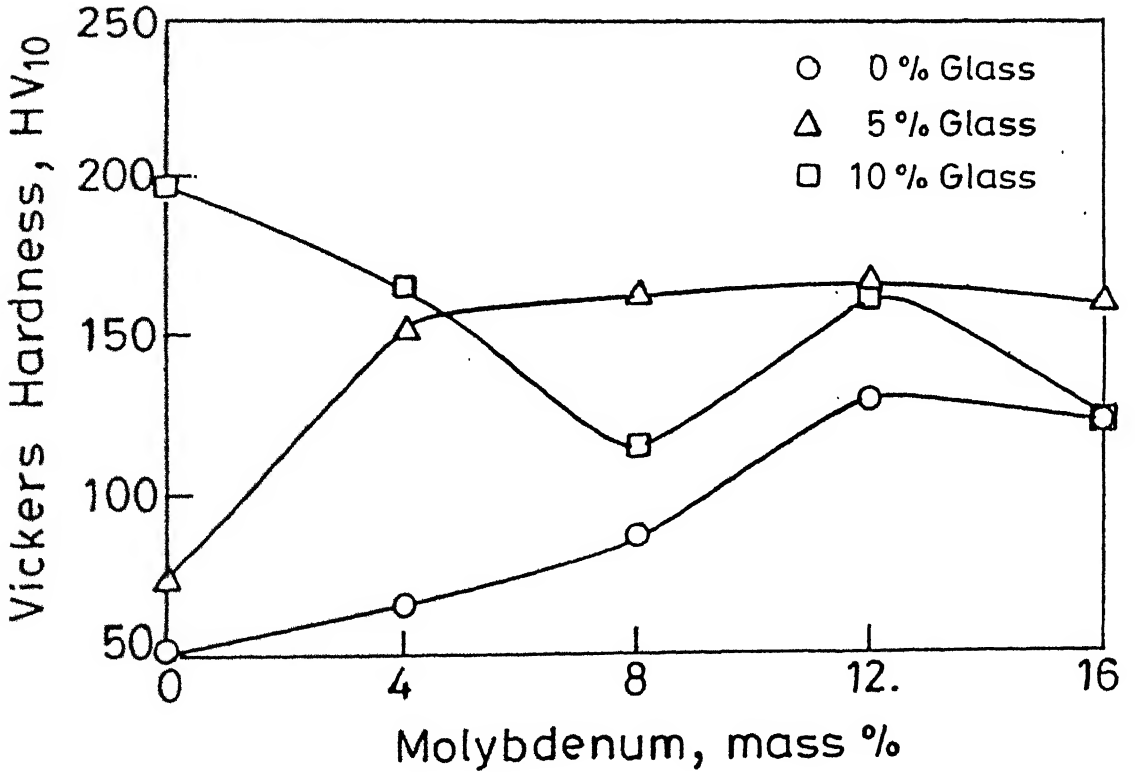

Fig. III.5 Variation of Vickers hardness with molybdenum content of alumina-molybdenum-glass composites.

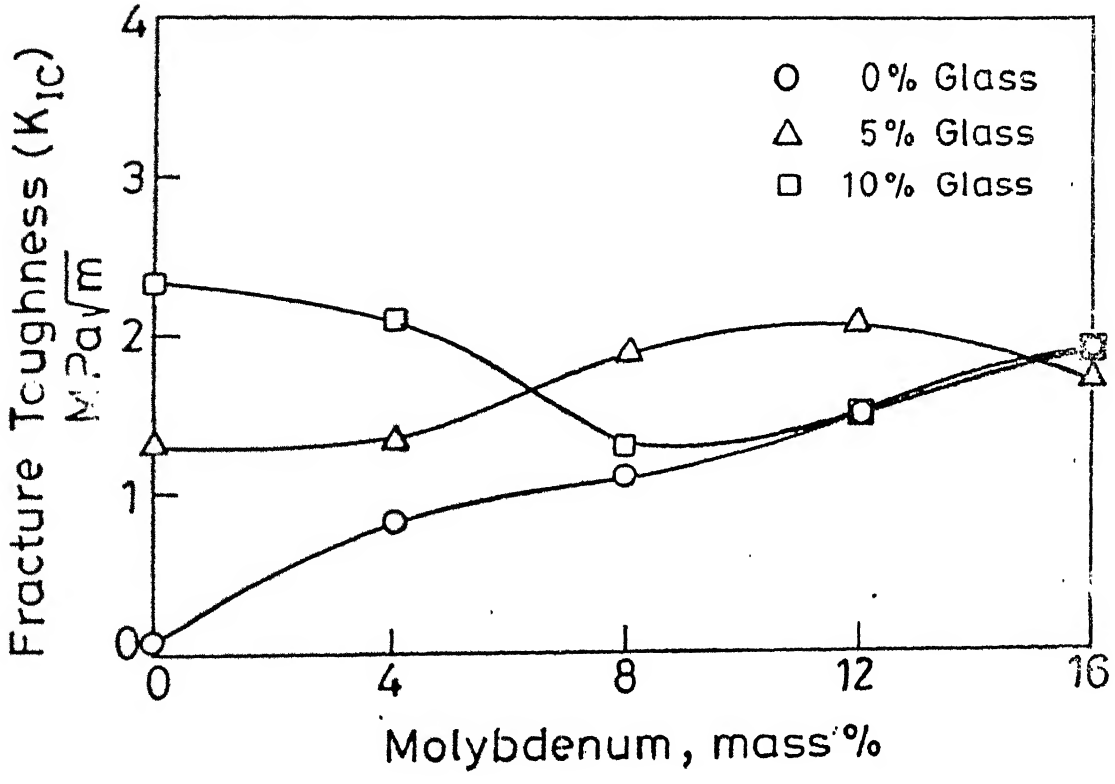

Fig. III.6 Variation of fracture toughness (K_{IC}) with molybdenum content of alumina-molybdenum-glass composites.

is shown in Fig. III.6. Fracture toughness (K_{IC}) was found to increase with increase in molybdenum content, which was found more significant for 0 mass % glass containing composites and least significant for 10 mass % glass containing composites. All the three mechanical properties measured, were found to have a maximum at alumina 10 mass % glass composition without any molybdenum.

III.4. SEM FRACTOGRAPHY:

Figures III.7 to III.9 show the secondary electron images of fractured surfaces of alumina-molybdenum composites containing 0, 5 and 10 mass % glass respectively. In all the compositions the fracture was purely intergranular and debonding of both alumina-alumina grains and alumina-molybdenum grains were seen. The shape of the alumina grains are platelike. It is also noticeable that the size of the alumina grains decreases in the presence of molybdenum particles. For any particular molybdenum content, it is apparent that the grain size of alumina increases with increase in the glass content.

III.5. X-RAY DIFFRACTION ANALYSIS:

X-ray diffraction patterns show only the presence of alumina and molybdenum (Fig.III.10-III.12). Formation of any other compound or phase change was not detected. In case of glass addition to alumina-molybdenum composites, the peak intensity was reduced. No broadening effect or peak shift, as such, was observed.

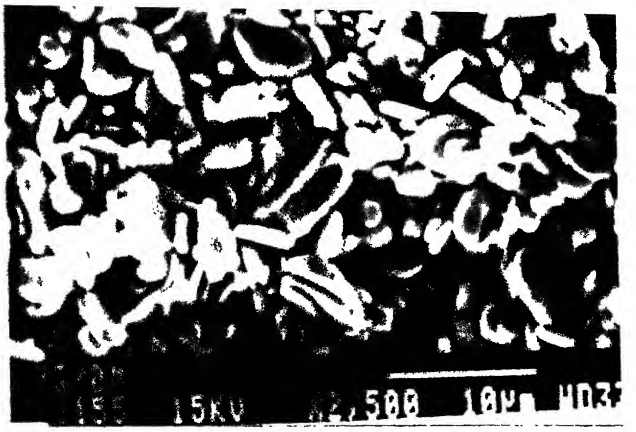

(a)

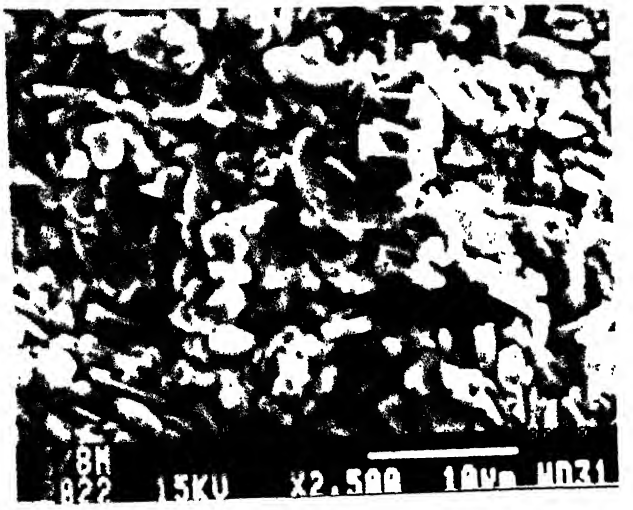

(b)

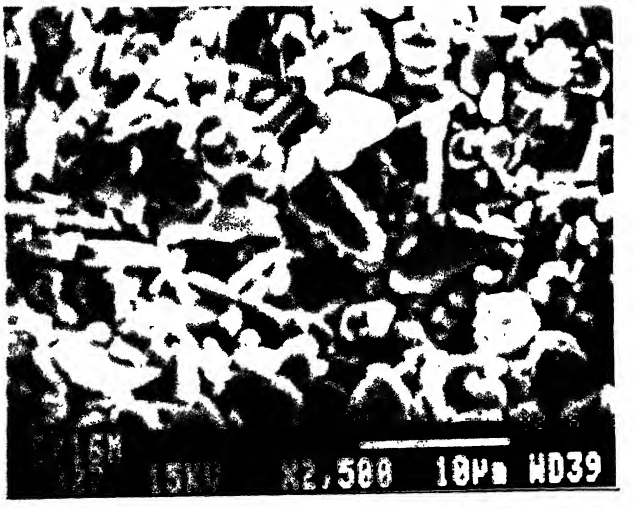

(c)

Fig. III.7 SEM fractographs of (a) alumina (b) alumina-8% molybdenum (c) alumina-16% molybdenum.

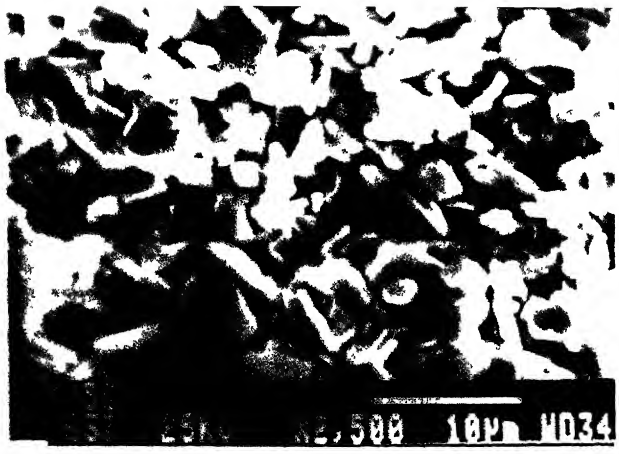

(a)

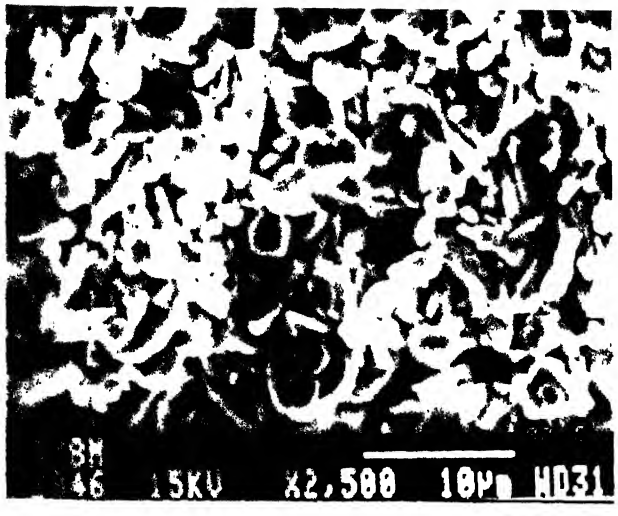

(b)

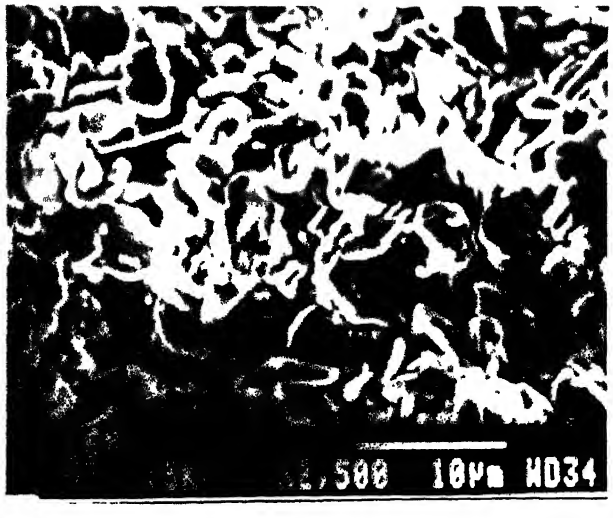

(c)

Fig. III.8 SEM fractographs of alumina-5% glass composites containing (a) 0% molybdenum

(a)

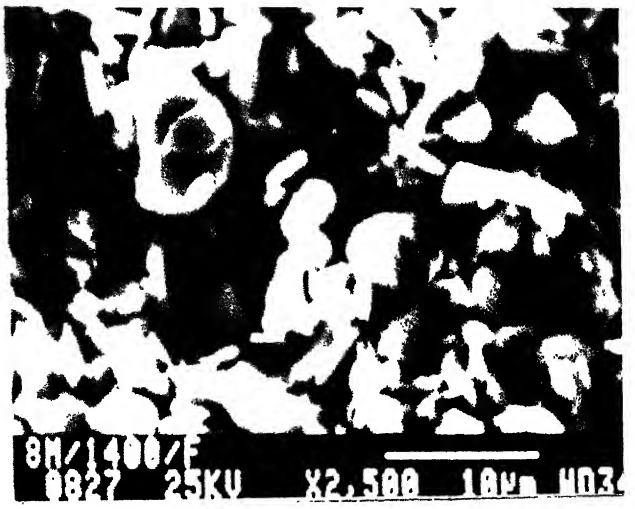

(b)

(c)

ig. III.9 SEM fractographs of alumina - 10% Glass composites containing (a) 0% molybdenum (b) 8% molybdenum (c) 16% molybdenum.

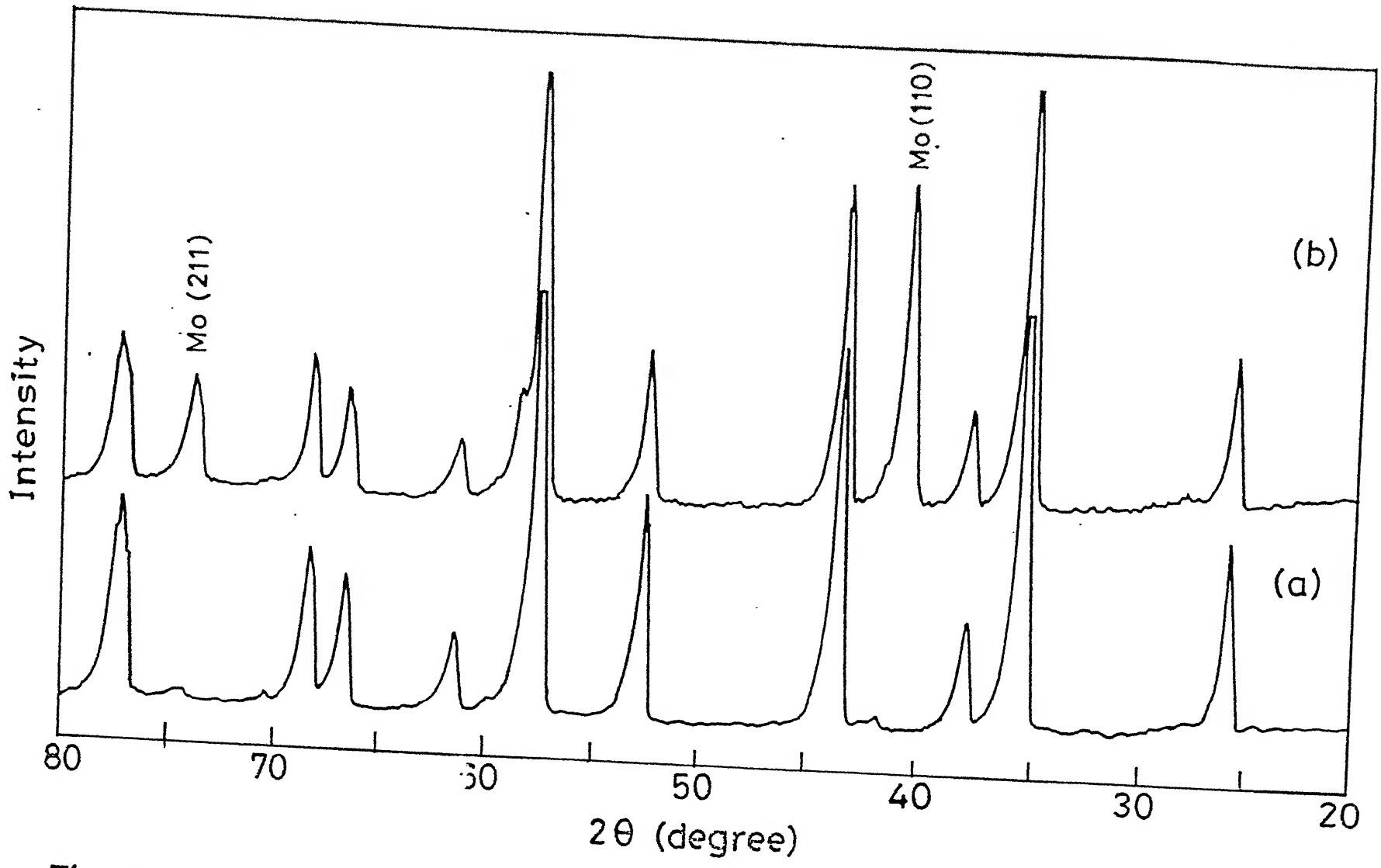

Fig. III.10 X-ray diffraction patterns of sintered (a) alumina (b) alumina-

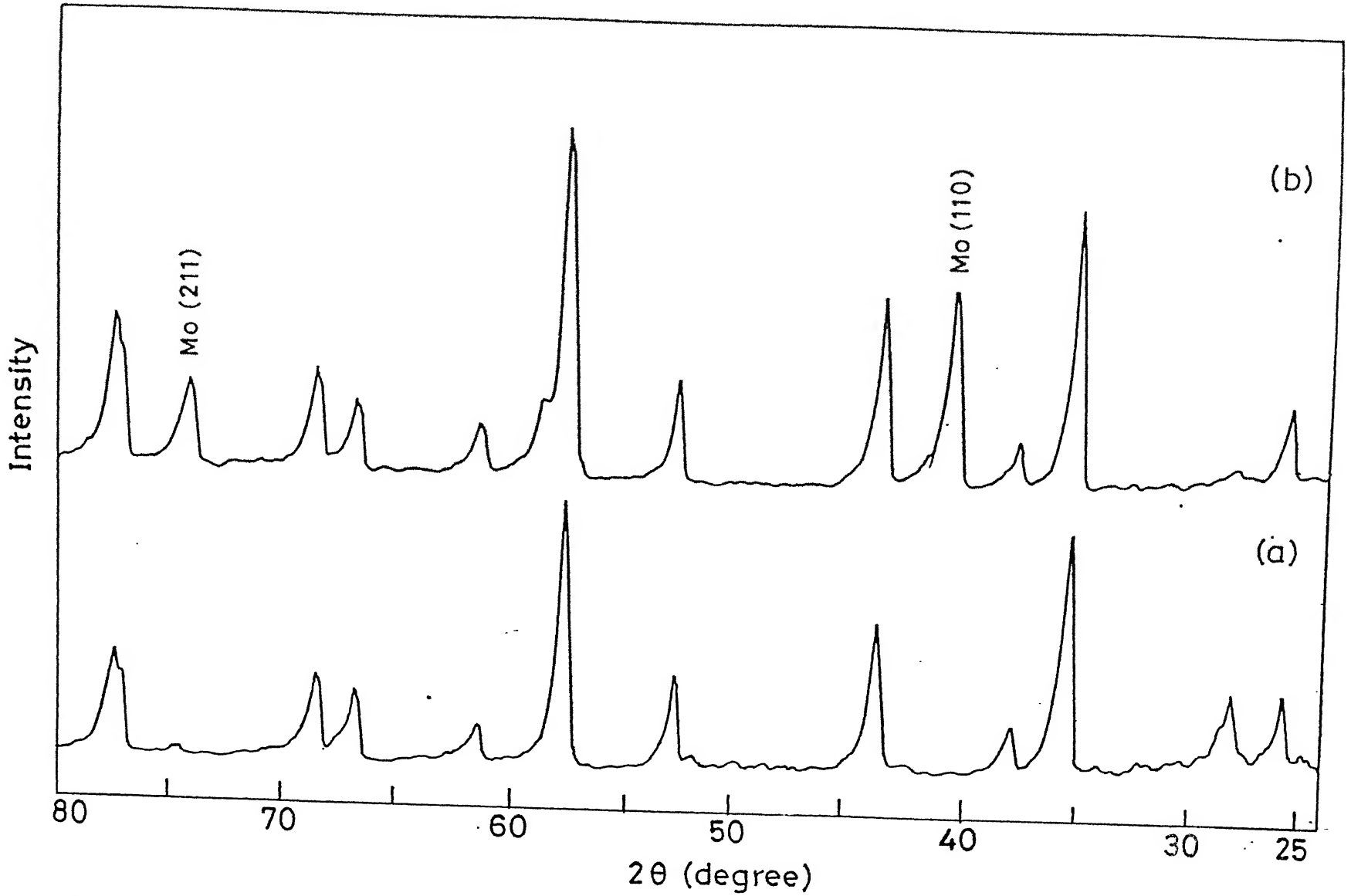

Fig. III.11 X-ray diffraction patterns of sinterered (a) alumina-5% glass (b) alumina-5% glass-8% molybdenum composites.

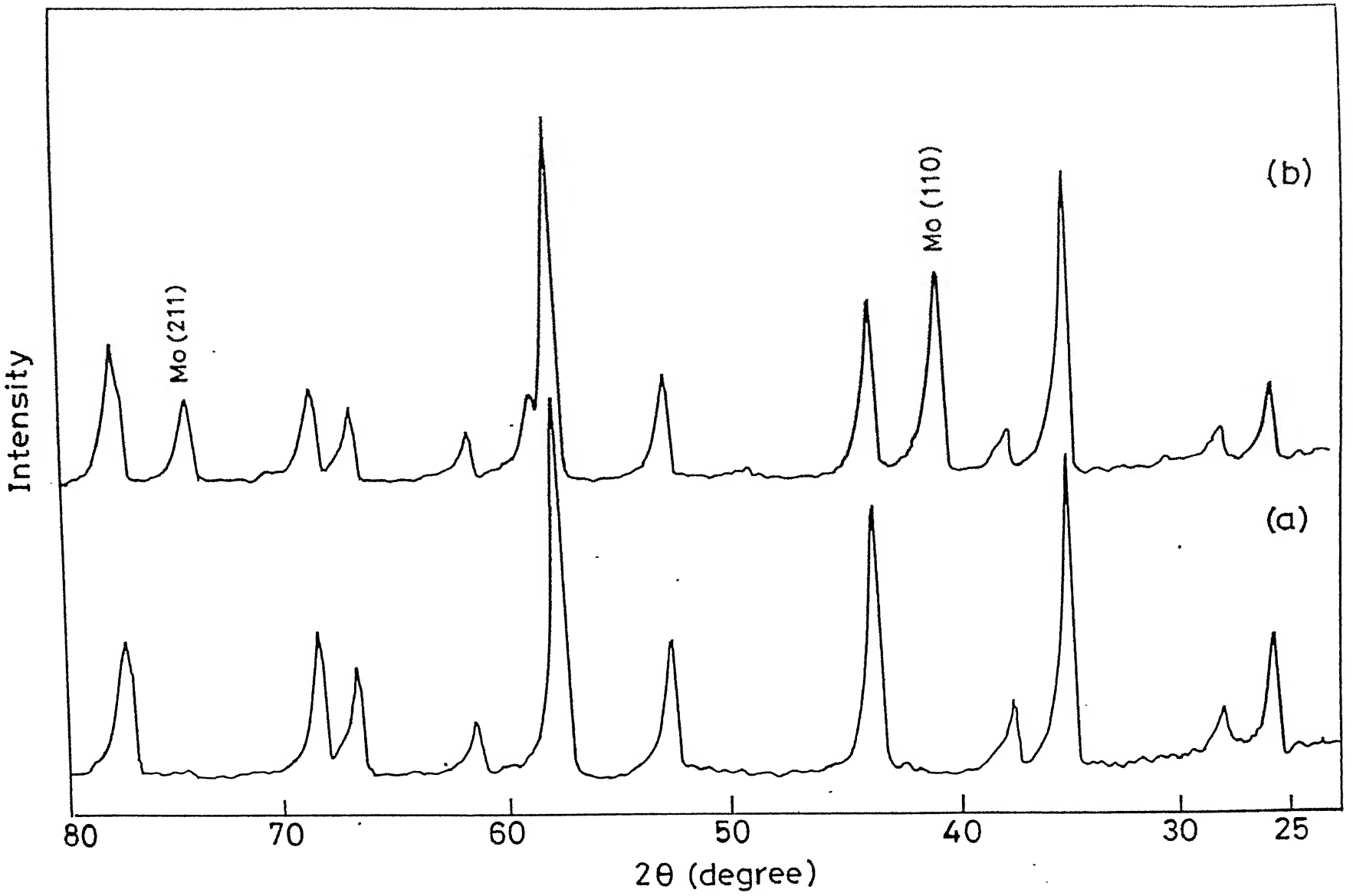

Fig. III.12 X-ray diffraction patterns of sintered (a) alumina -10% glass (b) alumina 10% glass -8% molybdenum composites.

PART-B: Solid State Sintered Al_2O_3-Mo Composites

III.6. SINTERED DENSITY:

The sintered density of aluminium-molybdenum composites was found to increase with molybdenum content of 8 mass % (Fig. III.13a). The sintered density has the optimum value of 89% theoretical for 8 mass % molybdenum, which decreases as the molybdenum content is still increased.

III.7. MECHANICAL PROPERTIES:

III.7.1. Vickers Hardness:

Vickers hardness of the composites was found to decrease with an initial increase in the molybdenum content from 0 to 16 mass % (Fig. III.13b). For 4 mass % molybdenum containing composites, Vickers hardness was found to have the maximum value of 650 VH_{10}.

III.7.2. Fracture Toughness (K_{IC}):

Molybdenum addition to alumina gave rise to an increase in the fracture toughness (K_{IC}) of the composites (Fig. III.13c). Upto 12 mass % molybdenum the fracture toughness (K_{IC}) of the composites was found to be increasing with increase in molybdenum content, above which no further increase was seen. The maximum fracture toughness obtained was a little above 4 MPa $\sqrt{m}$ for the alumina-12 mass % molybdenum composite.

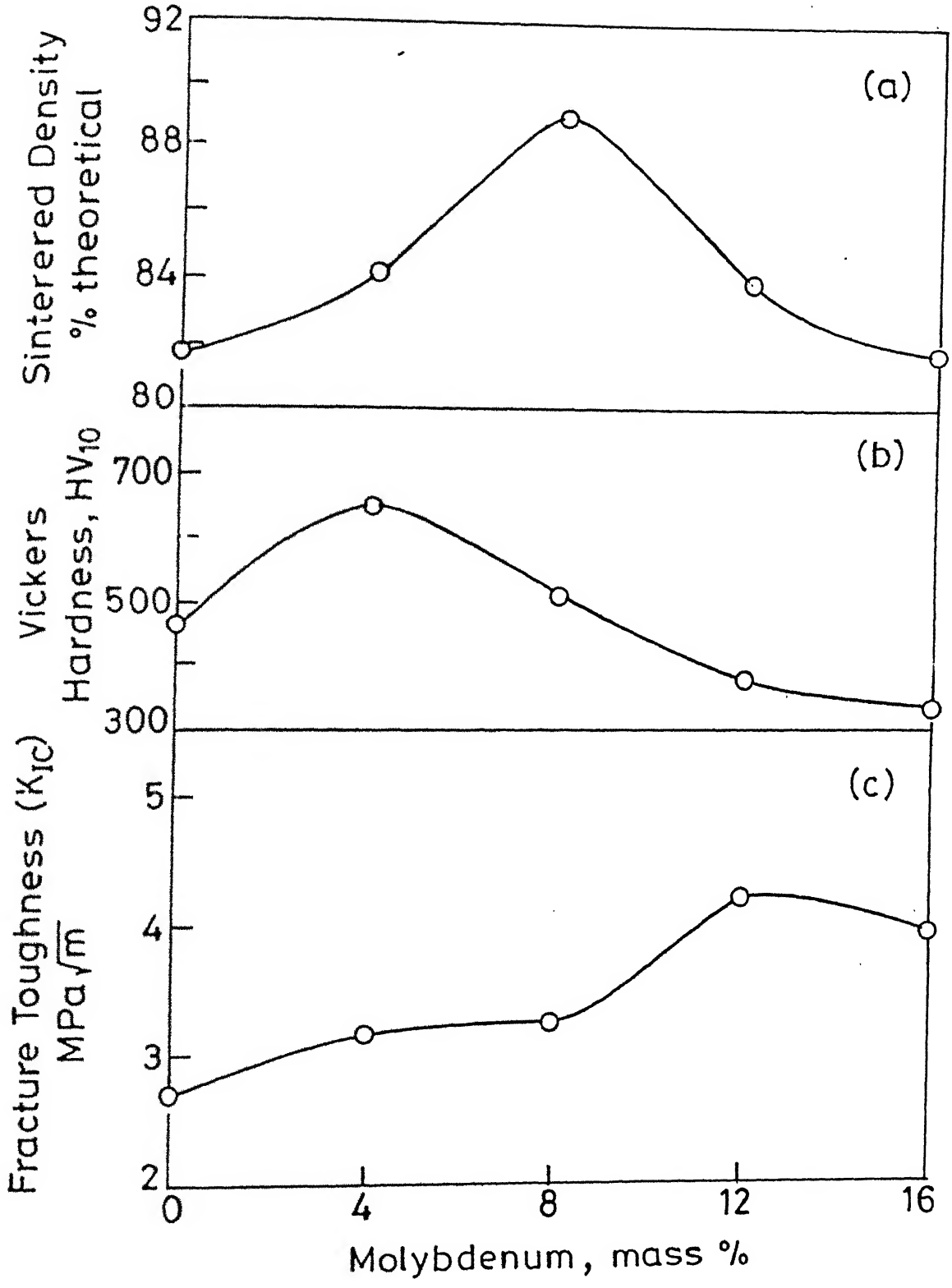

Fig. III.13 Variation of (a) sintered density (% theoretical) (b) Vickers hardness (c) fracture toughness (K_{IC}) with molybdenum content of alumina-molybdenum composites.

III.B. SEM FRACTOGRAPHY:

Secondary electron image of the fractured surface of the composites reveals significant grain growth of the alumina matrix (Figure III.14). Unlike the composites sintered at 1400°C, there was no significant grain refinement due to molybdenum addition to the composites. On the contrary, an enhanced grain growth was observed for alumina-16 mass % molybdenum composites as compared to others. The alumina grains were observed to be platelike similar to those described in Part A.

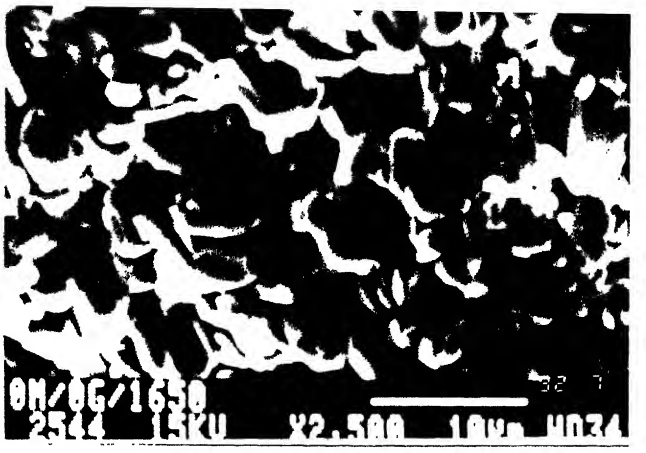

(a)

(b)

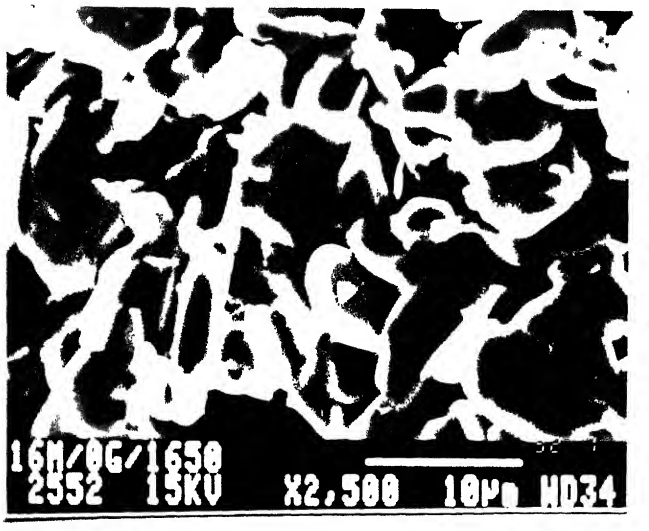

(c)

Fig. III.14 SEM fractographs of (a) alumina (b) alumina-8% molybdenum (c) alumina-

CHAPTER - IV

DISCUSSIONS

PART-A: Liquid Phase Sintered Al_2O_3-Mo Composites

The selection of the particular ternary glass system i.e. $CaO-Al_2O_3-SiO_2$ (CaO - 23%, Al_2O_3 - 15%, SiO_2 - 62%) as an additive in Al_2O_3 matrix is dictated by the fact that it corresponds to the lowest melting point (1170°C) among any of the compositions [31]. The initial sintering temperature of 1400°C for the alumina-glass densification was purposely selected at the higher side, so that the glass melt might be less viscous, thus promoting liquid phase transport process.

The processing of the present alumina-glass system is a typical example of non-reactive liquid phase sintering. Among various stages of liquid phase sintering it is obvious that the first stage i.e. particle rearrangement is very much operative as densification is enhanced with the increase in glass content upto 10 mass % (Fig. III.2). The role of solution reprecipitation stage has been suggested elsewhere [27] in such systems containing MgO additives. The penetration of polycrystalline alumina by glass does not appear to be significant in the current investigation as the initial green porosities of the compacts were pretty high (44% approximately). As the amount and composition of the glass melt does not vary during sintering resulting a maximum sintered density of 71% theoretical, the predominant mechanism for liquid phase

sintering is supposed to be particle rearrangement. Flaitz and Pask [34] did confirm such phenomena in dense polycrystalline alumina during the later stage of sintering, which impart some growth in the compact. The variation of sintered density with the amount of glass melt shows a maximum value which agrees with the result of Agrawal and Narasimhan [24].

The decrease in sintered density with increase in glass content above the optimum value of 10 mass % can be attributed to the presence of excess viscous glass melt which blocks the pore channel restricting the pore elimination. The necessary mechanism for shrinkage in the first stage of liquid phase sintering is center to center approach, where the driving force is the decrease in interfacial energy. The presence of excess viscous liquid inhibits the particle rearrangement process due to the sluggish spreading of the melt.

The addition of molybdenum to 0% glass and 5% glass compositions promotes densification as shown in Figure III.1. For still higher glass containing composites viz. 10 mass %, the densification is sluggish with the molybdenum addition. Mc Hugh et.al. [8] and Rankin et al. [9] have also confirmed the above fact in which pure alumina did densify better in the presence of molybdenum. It is also seen from the same figure that the enhancement of sintered density due to molybdenum addition is more effective for lower glass containing composites. This indicates that for higher glass containing composites viz. 10%, the interaction of molybdenum on alumina is retarded due to the presence of excess viscous glassy phase.

As regards the microstructure of the polycrystalline alumina is concerned, Song and Coble [30] has reported the origin and growth kinetics of liquid phase sintered alumina with dopants such as MgO, CaO or CaO + TiO_2. Their observation was platelike grains of alumina, which was also noticed in the present experiment (Fig.III.7-III.9). The author [30] established that the flat boundaries of platelike grains wetted with a liquid glass phase were basal planes. The grain coarsening with increase in glass content indicates that there is some extent of second stage liquid phase sintering viz. solution-reprecipitation. The driving force for the origin of platelike grain formation is the difference between solubility between growing and shrinking grains, due to conservation of anisotropic interfacial energy of alumina with the respective liquid phase. The increase in glass content in addition to densification increases the grain growth of alumina, similar to that observed by Agrawal and Narasimhan [24]. This indicates that the pores located at the grain boundary are swept away during grain boundary movement.

The addition of molybdenum to alumina decreases its grain growth rate by pinning the grain boundary, which agrees with the result of Mc Hugh et.al. [8] and Fedotov [13]. The continuation of grain refinement was not observed in 16% molybdenum containing composites due to the tendency of coalescence of molybdenum particle. The enhancement of densification of the composites due to molybdenum addition is because of the grain refinement which prevents pore entrapment. This may also be attributed to the decrease in

interfacial energy between alumina and molybdenum causing better bonding between the two.

To understand the liquid phase sintering more quantitatively, Kwon and Messing [25] recently proposed a liquid phase sintering map in which conservative condition for solution-reprecipitation was proposed by the basis of geometrical and kinetic factors.

The solubility of alumina in the glass melt was not confirmed from the present X-ray diffraction studies. There was no chemical reaction product detected in the sintered composites which confirms the result obtained by Kostic et.al. [28]. Singh [22] and Agrawal and Narasimham [24] did confirm that the apparent activation energy for densification decreases with increasing liquid content, because of the concurrent densification by rearrangement and solution-reprecipitation mechanisms. Based on the time exponent and activation energy measurements, Broklin and Platov [11] proposed that densification of an alumina glass system is controlled by diffusion during solution-precipitation.

The transverse rupture strength (TRS) of 0% glass containing composites is significantly increased with molybdenum addition as compared to that for 5% and 10% glass containing composites. This shows that the bonding between the alumina-molybdenum particle is stronger in the absence of the liquid phase. To improve TRS, the addition of glass seems more beneficial in case of the lower molybdenum containing compositions. This supports the earlier observation that

glass addition adversely affects the interaction of molybdenum on alumina. The increase in TRS with increase in molybdenum content of the alumina-molybdenum glass composites may be attributed to the decrease in grain size of alumina and increase in sintered density, which confirms the report of Mc Hugh et.al. [8].

The variation of Vickers hardness with molybdenum content of the composites follows the same trend as that of TRS. It is interesting to note that the results of Brokhin and Platov [11] are in variation to the present findings, such that they observed fall in sintered density and hardness of alumina with increase in molybdenum addition.

Fracture toughness (K_{IC}) of the sintered compacts varies in the same manner as that of sintered density with molybdenum content. As it is apparent from Figures III.3 to III.6, the role of glass addition on densification and the mechanical properties is more perceptible in lower molybdenum containing compositions. This might be attributed to the less degree of viscous drag in the molten glass, where rather little or no molybdenum was in suspension. The better mechanical properties of Al_2O_3 - 8%, Mo - 5% glass than other ternary compositions clearly menifests that there is ought to be an optimisation between the amount of molybdenum and glass. In other words, both the presence of glass melt as well as the grain size of alumina are contributing towards achieving the optimum properties.

PART-B: Solid State Sintered Al_2O_3-Mo Composites

The solid state sintering of alumina molybdenum composites sintered at 1650°C has considerably increased the densification with respect to that sintered at 1400°C. The sintered density enhancement due to molybdenum addition upto 8% may be attributed to the formation of strong bonding between alumina and molybdenum particles causing decrease in interfacial energy. Also mutual solubility upto a small extent at such high temperature between the two is not ruled out which may further increase the sintered density. Further increase in metal content, above 8%, decreases the sintered density which may be attributed to the coalescence of molybdenum particles. This indicates that an optimum quantity of molybdenum addition gives the maximum densification which supports the observations of Mc Hugh et.al. [8] and Fedotov [13].

As regards the microstructure of the composites, considerable grain growth has occurred due to the extensive solid state diffusion of alumina during the isothermal heating at 1650°C. It is apparent that the grain boundary pinning effect due to molybdenum particles no longer holds good at such an elevated sintering temperature i.e. 1650°C. As the alloy was sintered in air, the possibility of the oxidation of molybdenum in the oxides may not be ruled out. Mc Hugh et.al. [8] has reported the formation of an eutectic between MoO_3 and MoO_2, which might attribute in greater coarsening of high Mo-containing composites (Figure III.14).

The uniform increase in the fracture toughness (K_{1C}) with the molybdenum addition is an contrast with the Vickers hardness variation, where a peak was noticed at 4% Mo composition. This shows that molybdenum imparts ductilising effect over the brittle Al_2O_3 matrix. The nature of plot is similar to that for 1400°C sintered composites, with the distinction that the values are on the higher side.

The decrease in Vickers hardness with an initial increase as molybdenum is added to alumina, may be due to the fall in sintered density at higher molybdenum content.

CHAPTER - V

CONCLUSIONS

1. Alumina-calcium aluminosilicate glass (CaO - 23%, Al_2O_3 - 15%, SiO_2 - 62%) compacts when sintered at 1400°C, undergoes nonreactive liquid phase sintering, the predominant mechanism being particle rearrangement.
2. The addition of glass or molybdenum promotes densification and improves mechanical properties e.g. TRS, fracture toughness and Vickers hardness.
3. The maximum sintered density in case of alumina-glass composites is achieved with an optimum glass content of 10 mass %.
4. The alumina-molybdenum-glass composites containing 8% molybdenum and 5% glass yield maximum densification and mechanical properties.
5. The solid state sintered alumina-molybdenum composites have higher sintered density and mechanical properties than those of liquid phase sintered ones.
6. Molybdenum addition in case of liquid phase sintered alumina-glass composites decreases the matrix grain size while the reverse is true in case of glass addition to the alumina-molybdenum composites.
7. The alumina grains in case of liquid phase sintered composites showed platelike structure mainly because of the difference in the solubility between growing and shrinking grains.

3. In case of solid state sintering, the matrix grain size was found to increase with molybdenum addition which was contrary to liquid phase sintering.

REFERENCES

1. W.H. Gitzen (Ed.), Alumina as a Ceramic Material, Columbus, Ohio, The American Ceramic Society, 1970.

2. A.A. Griffith, "Phenomena of rupture and flow in solids", Phil. Trans. Roy. Soc., 221A (1920), 163-98.

3. N.J. Petch, "Cleavage strength in polycrystals", J. Iron and Steel Inst., 174 (1953), 25-38.

4. E. Dorre and H. Hubner, "Alumina", Springer-Verlag, Heidelberg, 1984.

5. F.F. Lange, "The interaction of crack front with a second phase dispersions", Phil. Mag., 22 (1970), 983-992.

6. A.G. Evans, "The strength of brittle materials containing second phase dispersions", Phil. Mag., 26 (1972), 1327-1344.

7. W.D. Kingery, "Metal ceramic interactions I, Fractures effecting fabrication and properties of cermet body", J. Am. Cer. Soc., 36 (1953), 362-365.

8. C.O. Mc Hugh, T.J. Whalen and M. Humenik, "Dispersion strengthened aluminium oxide", J. Am. Cer. Soc., 36 (1953), 362-365.

9. D.T. Rankin, J.J. Stiglich and D.R. Petrak, "Hot pressing and mechanical properties of alumina with Mo dispersed phase", J. Am. Cer. Soc., 54 (1971), 277-281.

10. B.S. Skiden, G.A. Fomina and I.A. Shipilov, "A study of the effect of processing factors on the properties of Al_2O_3-Mo cermet", Sov. Powd. Met. Metal. Ceram., (1978), 402-404.

11. N.S. Brokhin and A.B. Platov, "Preparation and microstructure of cermet Al_2O_3-Mo and ZrO_2-Mo", Sov. Powd. Met. - Metal Cer., 7 (1965), 576-580.

12. A.V. Fedotov and E.E. Lutskaya, "Sintering of cermets based on molybdenum, nickel and aluminium oxide in atmosphere of dry and moist hydrogen", Refractories, (1985), 30-34.

13. A.V. Fedotov, "Sintering of cermets based on molybdenum and alumina", Refractories, 1 (1987), 30-34.

14. S.V. Raman, "Variation of sintering kinetics and microstructure of alumina with molybdenum and chromium addition", J. Mat. Sc., 22 (1987), 3161-3165.

15. R.L. Coble, "Sintering of crystalline solids: I. Intermediate and final diffusion model", J. Ap. Phy., 32 (1961), 787-792.

16. H.F. Cahoon and C.J. Christensen, "Sintering and grain growth of alpha alumina", J. Am. Cer. Soc., 39 (1956), 337-344.

17. L. Johnson and I.B. Cutler, "Diffusion sintering II, Initial sintering kinetics of alumina", J. Am. Cer. Soc., 46 (1963), 545-550.

18. G.C. Kuczynski, L. Abernethy and J. Allan, "Sintering mechanism of aluminium oxide", W.D. Kingery (Ed.), Kinetics of High Temperature Process, New York, John Wiley and Sons, (1959), 163-172.

19. Yeh, T. Sung and M.D. Sacks, "Low temperature sintering of aluminium oxide", J. Am. Cer. Soc., 71 (1988), 841-844.

20. L. Xue and I.W. Chen, "Deformation and grain growth of low temperature sintered high purity alumina", J. Am. Cer. Soc., 72 (1990), 3518-3521.

21. W.D. Kingery, "Densification during sintering in the presence of a liquid phase I. Theory", J. Appl. Phys., 30 (1959), 301.

22. V.K. Singh, "Sintering of alumina in the presence of a liquid phase", Trans. Indian Ceramic Soc., 37 (1978), 55.

23. W.D. Kingery, E. Niki and M.D. Narasimhan, "Sintering of oxide and carbide-metal compositions in presence of liquid phase", J. Am. Cer. Soc., 44 (1978), 29.

24. G.N. Agrawal and M.D. Narasimhan, "Studies of eutectic sintering of MgO and Al_2O_3 ", Trans. Ind. Cer. Soc., 37 (1978), 79-86.

25. O.H. Kwon and G.L. Messing, "A densification map for liquid phase sintering", Paper presented at the 89th Annual meeting of The American Ceramic Society, Pittsburg, P.A., April 27, 1987 (Basic Science Division, Paper No. 49B-87).

26. P.L. Flaity, "Some aspects of liquid phase sintered alumina", Ph.D. Thesis, University of California, Berkeley, California (1982).

27. J.H. Hodge, "Effect of particle size distribution on the liquid liquid phase sintering of alumina", Ceram. Transac., 7 (1988), 415-435.

28. L. Kostic, C. Kis and S. Boskovic, "Liquid phase sintering of alumina", Powd. Met. Int., 19 (1987), 41-43.

29. W.A. Kaysser, M. Springler, C. Handwerker and J.E. Blendell, "Effect of liquid phase on the morphology of grain growth in alumina", J. Am. Cer. Soc., 70 (1987), 339-343.

30. H. Song and R.L. Coble, "Origin and growth kinetics of platelike abnormal grains in liquid phase sintered alumina", J. Am. Cer. Soc., 73 (1990), 2077-2085.

31. E.M. Levin, "Phase diagrams for ceramists", Am. Cer. Soc., Columbus, Ohio, 1956.

32. G. Arthur, J. Inst. of Metals, 83 (1954), 1329.

33. D.R. Larson and J.A. Coppola, D. .H. Hasselman and R.C. Bradt, "Fracture toughness and spalling behaviour of high alumina refractories", J. Am. Cer. Soc., 57 (1974), 417-421.

34. P.L. Flaitz and J.A. Pask, "Penetration of polycrystalline alumina by glass at high temperature", J. Am. Cer. Soc., 70 (1987), 449-455.